Journal of Magnetism and Magnetic Materials xx (xxxx) xxxx–xxxx

Contents lists available at ScienceDirect

Journal of Magnetism and Magnetic Materials

journal homepage: www.elsevier.com/locate/jmmm

Electronic and magnetic properties of bare armchair BC_2N nanoribbons

Hong Li[a,*], Xiang Xiao[a], Jun Tie[a], Jing Lu[b]

[a] College of Mechanical and Material Engineering, North China University of Technology, Beijing 100144, PR China
[b] State Key Laboratory of Mesoscopic Physics and Department of Physics, Peking University, Beijing 100871, PR China

ARTICLE INFO

Keywords:
First-principles calculations
BC_2N monolayer
Armchair-edged nanoribbons
Magnetic state

ABSTRACT

We present the electronic and magnetic properties of bare armchair BC_2N nanoribbons (ABC_2NNRs) in the view of density functional calculations. We consider three types of edge terminations with a width of 0.75 ~ 2.10 nm. All the investigated ribbons exhibit magnetic ground states with the magnetic moments mainly located on the edge C atoms. Room temperature accessible magnetic stabilities are obtained for ABC_2NNRs with NC-NC and NC-BC edge alignments. We find the ABC_2NNRs have various electronic structures, where half-metal, metal, and semiconductor are all acquired depend on the edge alignment and magnetic coupling state. The results show the ABC_2NNRs can be a promising candidate material in nanoelectronics and nanospintronics.

1. Introduction

Apart from the advancement in graphene related research, $B_xC_yN_z$ nanosheets [1–7], as a ternary 2D soft material, have gained their own momentum in nanoelectronics, optoelectronics, and energy storage applications [8]. The ternary $B_xC_yN_z$ hybrids between graphene and h-BN show very different but complementary properties to those of graphene and h-BN with tunable electronic properties ranging from semimetallic to insulating. As one of the most stable stoichiometry of $B_xC_yN_z$, BC_2N stoichiometry has strikingly different experimental band gaps of 23 meV [9], 2.0 eV [1], or indirect band gap of 1.6 eV [6]. Besides, in favor of device application, the carrier mobility of few-layer BC_2N is as high as 8×10^5 cm^2 V^{-1} s^{-1} [10].

Its one-dimensional (1D) nanostructures, named BC_2N nanoribbons (BC_2NNRs), possess various edge arrangements due to ample atomic alignments. This suggests a wide variety of electronic and magnetic properties in BC_2NNRs. Inspiringly, magnetism is predicted in BC_2NNRs with various edge configurations [11–15], distinct from their two-dimensional (2D) counterparts. This extends the applications of the BC_2NNR in spintronics. When truncated the BC_2N monolayer into armchair edge termination and keep the BN and C zigzag chain along the ribbon width at the same time, we get three edge types labeled as NC-NC, BC-BC, and NC-BC edge alignments. Wanlin Guo et al. have examined the same ABC_2NNRs with H-passivation, and half-metallic behavior is reported [11]. However, the magnetism is not stable at room temperature.

In this study, we examine the structure, stability, electronic, and magnetic properties of the bare ABC_2NNRs with density functional theory (DFT) simulations. Three types of edge terminations, *i.e.*, NC-NC, CB-CB, and NC-CB, with a ribbon widths range from 0.75 to 2.10 nm are studied. Room temperature accessible magnetic stabilities are obtained for ABC_2NNRs with NC-NC and NC-BC edge alignments. We recover half-metallic, metallic, and semiconducting properties in ABC_2NNRs depend on the edge alignment and magnetic coupling state.

2. Models and methods

The C atoms and BN pairs form zigzag atomic chains along the [010] direction in the theory predicted most stable configuration of BC_2N sheet as inset in Fig. 1, which possesses the most extensive number of C-C and B-N bonds [16–19]. With this BC_2N monolayer, we truncate it into armchair nanoribbons while keep the BN and C zigzag chains along the ribbon width. Thus, we get three types of edge terminations. We denote an ABC_2NNR with N_A dimer lines as N_A-ZBC_2NNR. The ribbons with odd N_A have edge arrangement NC-NC and CB-CB, while those with even N_A have edge arrangement NC-CB as shown in Fig. 2. With a 2×1×1 supercell, we consider six types of edge magnetic ordering for each ribbon as given in Fig. S1. In all the models, a vacuum of 30 Å is adopted to avoid the periodic interaction between its replicas.

We perform spin-polarized first-principles calculations based on the density functional theory (DFT) as implemented in the DMol^3 package [20]. The generalized gradient approximation (GGA) of Perdew-Burke-Ernzerhof (PBE) form [21] is chosen for the exchange-correlation functional. We use a numerical atomic orbital basis set plus a d-type polarization function (DNP) to expand wave functions. The global orbital cutoff energy for each element is set to 5.1 Å. The Brillouin-zone integration is sampled by 5×1×1 Monkhorst-Pack grids

* Corresponding author.
E-mail address: lihong@ncut.edu.cn (H. Li).

http://dx.doi.org/10.1016/j.jmmm.2016.10.156
Received 11 October 2016; Received in revised form 29 October 2016; Accepted 29 October 2016
Available online xxxx
0304-8853/

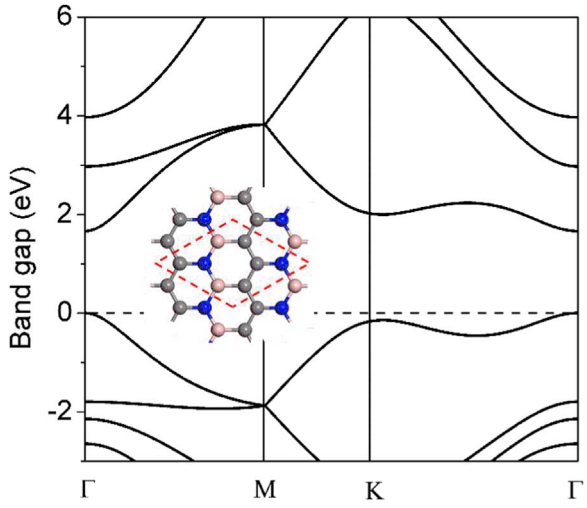

Fig. 1. Band structure of the BC_2N sheet. The Fermi level denoted by the black dash line is set to zero. Insert is the fully optimized BC_2N sheet with the red dash line quadrilateral indicating its unit cells. Small gray, blue and pink spheres denote carbon, nitrogen and boron atoms, respectively. (For interpretation of the references to color in this figure legend, the reader is referred to the web version of this article.)

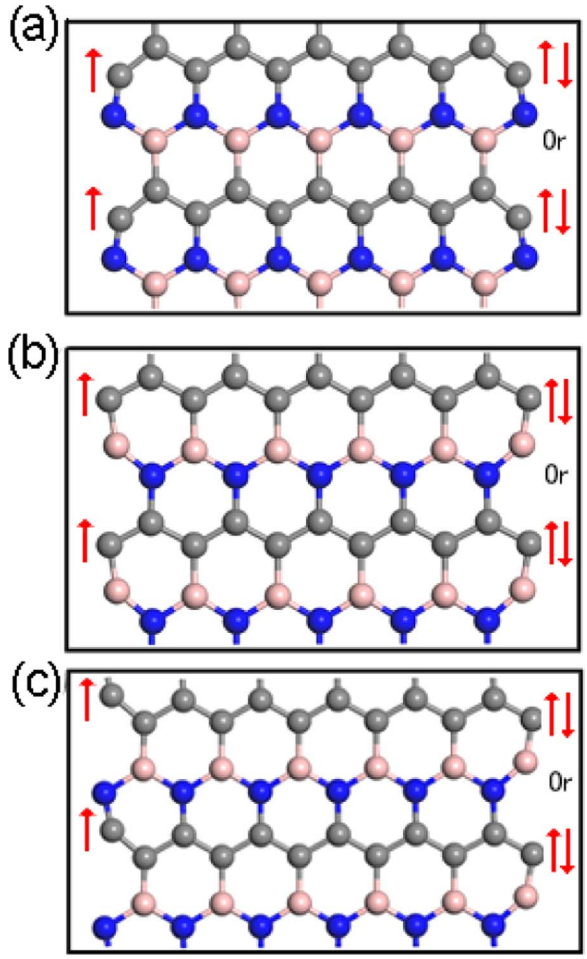

Fig. 2. Atomic structures of the fully optimized (a) NC-NC 11-ABC_2NNR, (b) CB-CB 11-ABC_2NNR, and (c) NC-CB 12-ABC_2NNR. The red arrows denote the spin distributions for the ground states. Small gray, blue and pink spheres denote carbon, nitrogen and boron atoms, respectively. The black solid rectangles indicate the 2×1×1 supercells of the ABC_2NNRs. (For interpretation of the references to color in this figure legend, the reader is referred to the web version of this article.)

[22] for atomic structure relaxation with a convergence threshold of 1.0×10^{-6} Ha on the energy and 0.001 Ha/Å on the maximum force. Electronic and magnetic properties are then studied on the optimized geometries with 25×1×1 k-points.

3. Results and discussions

Analogous to their all carbon analog graphene, the BC_2N monolayer forms strong planar hexagonal honeycomb structure as inset in Fig. 1. The binding energy of the BC_2N sheet is −7.24 eV/atom, larger than that of graphene (−7.91 eV/atom) but less than that of BN sheet (−7.03 eV/atom). This result indicates that the BC_2N sheet is less stable than graphene, but should be more stable than BN sheet. As shown in Fig. 1, the BC_2N sheet is a nonmagnetic semiconductor with a direct band gap of 1.66 eV at Γ point, in good agreement with previous studies [11,15]. Due to the analogous structure, relative stability, and moderate band gap, the BC_2N sheet is considered as an excellent complement to graphene and BN sheet for nanoelectronic applications.

The optimized atomic configurations of the bare NC-NC 11-, CB-CB 11-, and NC-CB 12-ABC_2NNRs are given in Fig. 2a, b, and c, respectively. The edge bonds change from the inner bonds depend on the edge type. At NC edge, the edge C atoms move inward a bit, and the NC bonds shorten obviously by 0.16 Å. Whereas at BC edge, the edge B atoms move inward a bit, and the BC bonds shorten obviously by 0.12 Å. For details, we give all the edge bond lengths for the NC-NC and CB-CB 11-ABC_2NNR and the NC-CB 12-ABC_2NNR in Table S1.

Ground states are then carefully examined with considering one nonmagnetic configuration and six spin coupling configurations for each ABC_2NNR, *i.e.*, each edge can be ferromagnetic or anti-ferromagnetic ordering as shown in Fig. S1. All the investigated ABC_2NNRs have magnetic ground states, and the spin distributions are similar. For demonstration, we mark the magnetic orderings of NC-NC 11-, CB-CB 11-, and NC-CB 12-ABC_2NNRs with red arrows in Fig. 2a, b, and c, respectively. The magnetic moments mainly located on the edge C atoms, and the spins are ferromagnetic coupling for each edge. While for the spin coupling on the opposite two edges, ferromagnetic and anti-ferromagnetic coupling are degenerate in energy.

To investigate the stability of these ABC_2NNRs, we define the binding energy (E_b) as,

$$E_b = (E_{total} - n_i E_i)/N$$

where E_{total} and E_i are the total energy of the optimized ABC_2NNRs at ground states and the atomic energies of the contained element i (i= B, C, and N), respectively. n_i and N denote the number of the contained i element and the total atom number, respectively. According to the definition, negative values represent thermal stability of the ribbons, and a smaller value means a more stable status. The binding energies of all the bare ABC_2NNRs with different edge arrangement and ribbon width (0.75–2.10 nm with N_A =7–18) are given in Fig. 3a. The E_b of its 2D counterpart is given for comparison, denoted by a red horizontal dash line. We find that the stabilities of the ABC_2NNRs improve with increasing ribbon widths. As to the similar ribbon width, the stabilities decrease in the order of the edge arrangement: NC-NC > NC-CB > CB-CB. All the values of E_b are given in Table S2.

Fig. 3b gives the energy differences per edge C atom between the nonmagnetic and magnetic states with respect to the ribbon width for the bare ABC_2NNRs. In general, the energy differences decrease in the order of the edge arrangement: NC-NC > NC-CB > CB-CB, at similar ribbon width. We can see that the energy differences of NC-NC ABC_2NNRs first increase rapidly (10 meV) to 81 meV (N_A =7 and 9) and then become constant (less than 1 meV) with ribbon width N_A =9–17. The trend with width is similar for NC-BC ABC_2NNRs, *i.e.*, the energy differences first increase rapidly (14 meV) to 28 meV (N_A =8 and 10) and then increase slowly (in a step of 2–3 meV) with N_A =10–18. As for BC-BC ABC_2NNRs, the energy differences first decrease rapidly (10 meV) to 14 meV (N_A =7 and 9), then increase slowly (in a